# LASER GENERATED GOLD NANOPARTICLES FOR MASS SPECTROMETRY OF LOW MOLECULAR WEIGHT COMPOUNDS

**Aneta PŁAZA-ALTAMER[1*], Artur KOŁODZIEJ[1], Joanna NIZIOŁ[2] and Tomasz RUMAN[2]**

[1] Doctoral School of Engineering and Technical Sciences at the Rzeszów University of Technology, 8 Powstańców Warszawy Ave., 35-959 Rzeszów, Poland

[2] Rzeszów University of Technology, Faculty of Chemistry, 6 Powstańców Warszawy Ave., 35-959 Rzeszów, Poland

[*]Corresponding author: a.plaza@prz.edu.pl, 178651310

Abstract: Preparation of gold nanoparticles (AuNPs) by pulsed fiber laser (PFL) laser generated nanomaterial (LGN) with the use of 2D galvo-scanner (2D GS) is described. The procedure of covering of custom-made stainless steel MALDI targets containing studied objects via nebulization is also presented. Examples of application of new method (PFL-2D GS LGN and nebulization) in laser desorption/ionization mass spectrometry (LDI MS) analyses are shown. These include tests with amino acids and also low molecular weight polymer.

**Keywords:** gold nanoparticles; laser generated nanomaterial; low molecular weight compounds; mass spectrometry; matrix-free laser desorption/ionization; surface-assisted desorption/ionization.

## 1. Introduction

The development of matrix assisted laser desorption/ionization in mass spectrometry (MALDI-MS) is attributed to Tanaka et. al [1]. Due to its soft ionization potential, MALDI is one of the most selective, sensitive and efficient mass spectrometry methods. This allows it to be widely used for the analysis of ionic high-molecular weight compounds such as peptides, proteins [2], synthetic polymers [3] or polysaccharides [4], but it is also possible to detect low molecular weight (LMW) compounds such as lipids [5,6]. However, a disadvantage of MALDI which prevents it from being used too frequently for the detection of LMW compounds (MW <1000 Da) is the need to use MALDI matrices, which are low molecular weight organic acids that generate a variety of matrix-bound ions during the desorption/ionization process. The suppression of the analyte peaks then occurs, which complicates the spectra and significantly hinders the analysis of the tested compounds [7–9].

In part, the problems outlined have been resolved by developing the surface ionization assisted mass spectrometry (SALDI) technique. SALDI uses target plates coated with various nanostructures [6,10,11]. The nanoparticles used simplify the mass spectrum by reducing spectral interferences. Sample preparation is also the much simpler step demanding only applying the sample to the target plate [12]. What is more, advantage of using nanoparticles (NPs) is the reduction of the "sweet-spot" effect and very good point-to-point reproducibility [11].

Nanoparticles can be made by chemical, physical or biological methods [13,14]. The most commonly used methods for obtaining nanoparticles for MS is chemical reduction [12,15,16]. However, this approach raises a number of problems. One of them is the chemical purity of the obtained suspension. The necessity to use substances for chemical reactions, such as metal precursors, reducing agents, stabilizers, and oxidized products, make them a source of reagent-related ions and generate numerous interfering signals [17–19]. Another way NPs can also be obtained by breaking up a larger structure, for example with a laser, which is classified as physical method [13,14]. The method of generating nano-

particles by means of a laser (LGN) has many advantages, owing to which the obtained NPs are successfully used in mass spectrometry [20–22]. LGN uses pulsed laser irradiation to ablate a target from a solid material immersed in a liquid, ejecting NPs from the plasma cloud into the surrounding solution. This method allows for the production of a nanoparticle suspension of relatively high chemical purity, due to the lack of necessity to use stabilizers and reducing agents required in the chemical reduction method [20,23–25].

The most popular method of laser mass spectrometry is MALDI, which uses low molecular weight organic matrices such as 2,5-dihydroxybenzoic acid (DHB), sinapic acid (SA) or α-cyano-4-hydroxycinnamic acid (CHCA). Unfortunately, the acidic nature of the matrix solutions can make the analysis of various compounds difficult. Moreover, MALDI is the most useful for ionic compounds, and due to numerous matrix signals in the *m/z* <1000 range, low mass accuracy, unreliable calibration and the "sweet spot" effect, it is rarely used for testing low-molecular compounds [26].

Most of above-mentioned MALDI problems may be solved by using metal nanoparticles, for example gold ones, as a desorption/ionization agents [6,12,27,28]. Since the publication of Russell's work on a method for obtaining controlled-size gold nanostructures, they have become increasingly used [29], which is confirmed by an extensive review of Abdelhamid and Wu [30]. So far, various techniques have been introduced to synthesize AuNP, including chemical, physical and biological. However, the most commonly used method is the chemical reduction, which requires two substances: a metal salt precursor and a reducing agent. In addition, almost all treatments also contain a stabilizer such as capping agent preventing NPs aggregation. The reaction involves the reduction of $Au_3^+$ to elemental gold by electron transfer under various conditions. Among the many gold precursors, we can distinguish chloroauric acid [31] or chloro(trimethylphosphite)gold(I) [12]. In turn, the role of the reducing agent is often assumed by sodium borohydride ($NaBH_4$), sodium citrate, hydrogen peroxide or ascorbic acid [13,32]. The type of the used precursor and reducer affects the properties and size of the AuNPs obtained [31].

Preparation and application of gold nanoparticles by chemical reduction method for laser mass spectrometry was presented by Tseng and Su [33]. Authors used $HAuCl_4$ as the metal precursor and sodium borohydride as the reducing agent. The obtained nanoparticles were used as templates in LDI MS for the detection of low molecular weight neutral carbohydrates such as glucose, ribose, maltose, and cellobiose. The mass spectra present mainly sodium and potassium adducts of the mentioned compounds. However, mass spectrum of mixture glucose, maltose and ribose shows a lot of interfering signals.

The above-mentioned problems were partly solved by Amendola and co-workers, who were the first to demonstrate a method for producing nanoparticles by laser ablation synthesis in solution (LASiS) and their applicability as a matrix for LDI MS [19]. Due to the simplicity of the method, the synthesis of nanoparticles with the use of laser ablation in a solution allows to save time while providing suspensions of relatively high chemical purity compared to chemical methods. The mass spectra with nanoparticles generated by the LASiS method have a low chemical background, which simplifies the analysis of the tested compounds. In addition, LASiS enables the production of NPs from a wide variety of metal alloys.

In last year publication, for the first time, 1064 nm pulsed fiber laser (PFL) with 2D galvanometer scanner (2D GS) is shown as a very good source of silver-109 nanoparticles [20]. This study describes a new method of production of chemically pure gold nanoparticles in suspension with an application method for covering of studied objects or surfaces. Laser generated gold nanoparticles are shown to be highly useful for LDI mass spectrometry. This work presents LDI MS results for test compounds such as amino acids and polymers.

## 2. Results and discussion

### 2.1. PFL 2D GS LGN of AuNPs

In this work, LGN has been used to obtain chemically pure gold nanoparticles. Nanoparticles were generated by pulsed 1064 nm fiber laser with galvoscanner head scanning of ablated surface. The experimental setup for the AuNPs preparation is shown in Fig. 1A. For fast synthesis of nanoparticles, high-frequency (60 kHz), high pulse energy (up to 1 mJ/pulse) laser was used. However, in order to

avoid unwanted thermal effects such as melting, solvent boiling and oxidation of solvent and also of nanoparticles, two-dimensional (2D) galvo-scanner (GS) was used. Galvo-scanner head with f-theta lens attached to fiber laser allowed for precise and very fast shifting of focused laser beam on the surface of ablated gold plate.

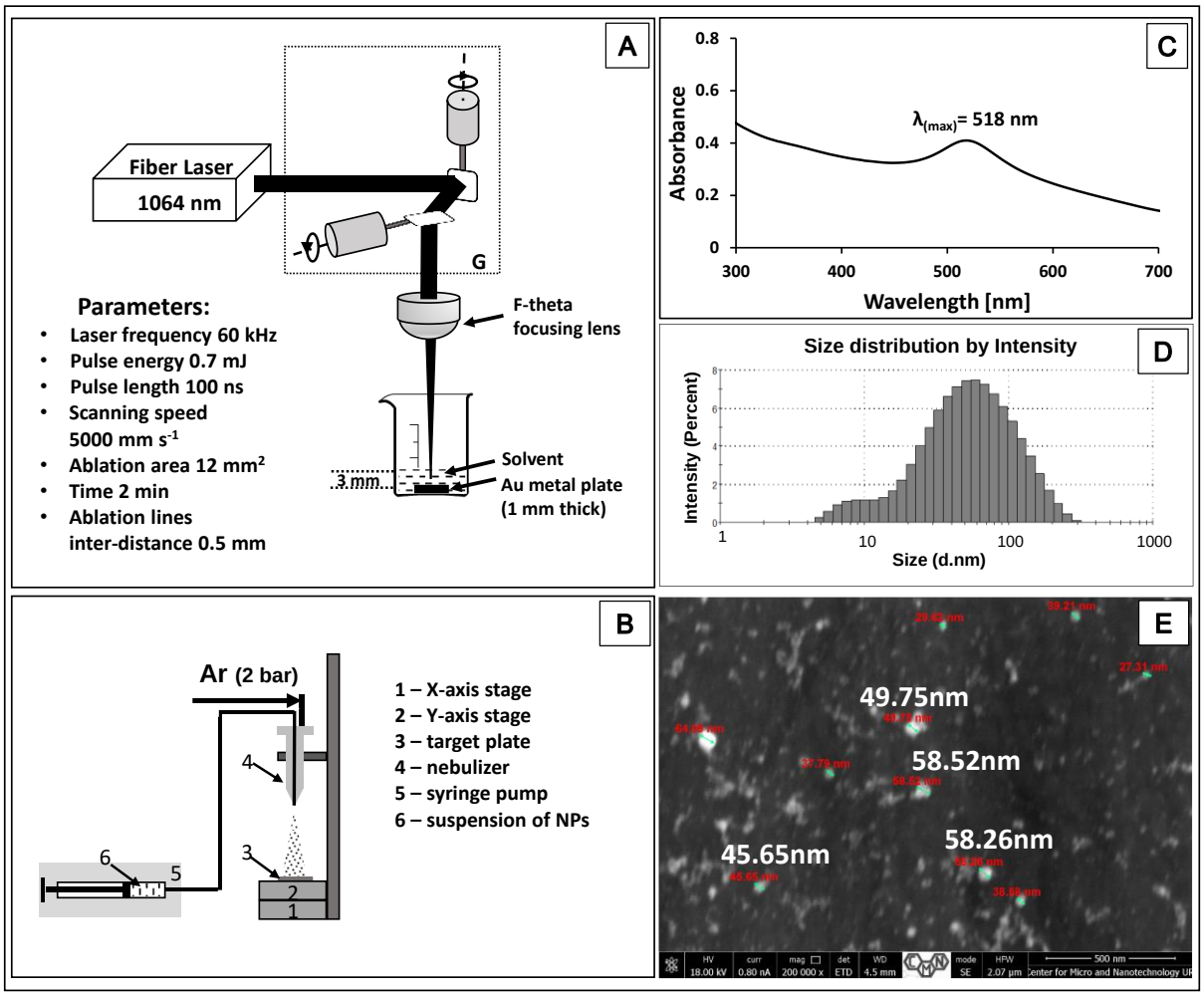


Fig 1**.** Laser ablation setup for the preparation of AuNPs (A); G – 2D galvanometer laser scanner. Down panel (B) presents setup for nebulization of nanoparticles. Panel C presents UV-VIS spectrum of AuNPs suspension in mixture solvents isopropanol and water (1:1 v/v). Panel D shows results of DLS measurement of Au nanoparticles hydrodynamic size distribution by intensity. E – High resolution SEM image of target modified with AuNPs generated by PFL 2D GS LGN.

First, the prepared nanoparticles were examined using UV-VIS spectroscopy, which allows determination of the size and shape of NPs. The vibrations of metallic electrons caused by particular wavelengths of light produce an effect known as surface plasmon resonance (SPR). It is related to the given size and shape of gold nanoparticles, as well as to their chemical environment. The literature describes that as the AuNPs diameter increases, the absorbance band shifts towards longer wavelengths and also widens [34]. The UV-VIS spectrum obtained for PFL 2D GS LGN AuNPs is presented in Fig. 1C. The UV-VIS spectrum of the post-reaction AuNP suspension recorded after 3 minutes of synthesis shows a local maximum at 518 nm, which suggests that the size of most nanoparticles is approx. 12 nm. However, an asymmetrical broadening of the SPR towards longer wavelengths, characteristic of the spheroidal particle fraction, can be observed. The presence of spheroids may indicate particle aggregation processes taking place in the suspension [34,35].

Figure 1D presents results of dynamic light scattering (DLS) measurement result of AuNPs size distribution by intensity after few minutes after preparation of suspension. DLS chart of the size distribution by intensity indicates the highest content of nanoparticles around 60 nm in diameter, with a distribution ranging from 5 to 120 nm. High resolution scanning electron microscope image of modified target (Fig. 1E) also confirms that individual nanoparticles are in roughly round/spherical shape and are

of 37-64 nm size. A number of HRTEM and DLS results on size measurements of gold nanoparticles obtained with LGN present similarly size. DLS results suggest bigger nanoparticles as judged from UV-vis spectrum. Most probably, this is due the fact that the nanoparticle suspension used for the DLS measurement was prepared in a different solvent than the one optimized for LGN. Many studies show the effect of solvent on the size of nanoparticles obtained [34,35].

The use of nanoparticles in LDI MS requires an appropriate method of application to the surface containing the tested object. One of the approaches using AuNPs as a matrix is dry metal sputtering to obtain a homogeneous layer with minimal or no lateral migration of the analyte. However, this method requires an appropriate spraying system and is therefore rarely used [36]. For our LDI MS measurements, 0.5 µl of each of solution of alanine, arginine, histidine, lysine, methionine, phenylalanine, serine and tyrosine and PPG polymer was applied to a stainless-steel plate and air-dried. The plate with all test objects was placed on the table of the translation system as shown in Figure 1B. Aliquots of colloidal gold (1 mL) were sprayed three times onto the sample. Each portion was injected into the nebulizer at a constant rate of 250 µl/min. The entire nanoparticle nebulization process was controlled by a computer using a sequence of movements aimed at evenly covering the target plate. The LDI MS spectrum of AuNPs produced by PFL 2D GS LGN and deposited on the surface of stainless steel of target plate by nebulization is shown in Figure 2A. Mass spectrum made in 80-1500 *m/z* range contains virtually only gold ion peaks of $Au^+$ to $Au_5^+$ composition. Various amino acids as low molecular weight compounds were tested to verify the potential of ionization of organic compounds with the gold nanoparticles obtained with PFL 2D GS LGN.

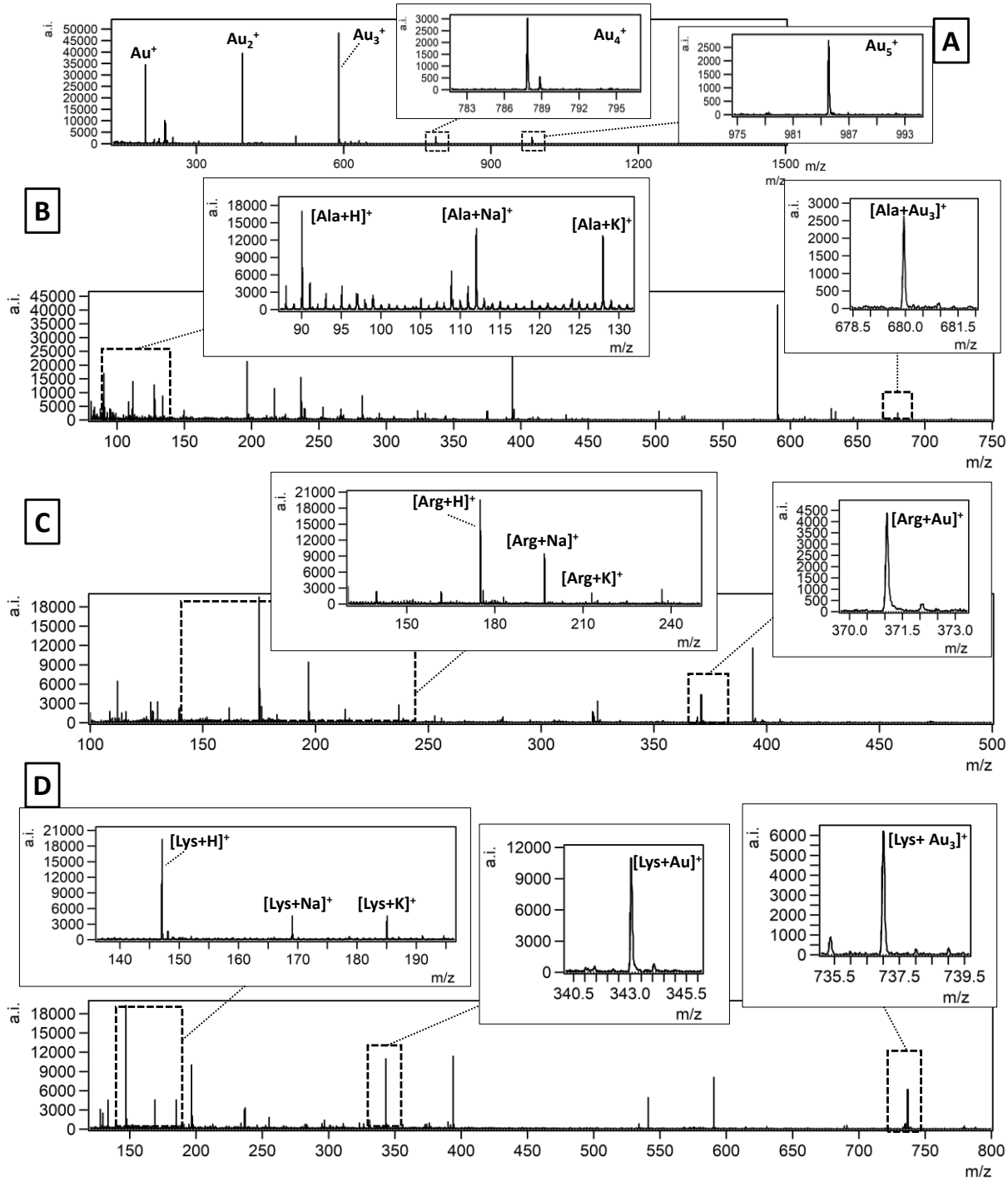


Fig 2. LDI MS positive reflectron mode spectrum of target plate covered with AuNPs generated by PFL 2D GS LGN (A). Others panels present LDI MS spectra fragments for alanine (B), arginine (C) and lysine (D) of 1 mg/mL concentrations deposited on target plate and covered with gold nanoparticles obtained with PFL 2D GS LGN.

The first analyzed compounds were alanine, arginine and lysine (Fig. 2). All listed compounds were found mainly as protonated adduct. Other adducts such as sodium, potassium as well as with $Au^+$ or $Au_3^+$ ions were also observed, but their intensities were significantly lower. For alanine (Fig. 2B), the highest S/N ratio equals 124 was observed for $[C_3H_7NO_2+H]^+$ adduct with *m/z* 90.0847. Ion of formula $[C_3H_7NO_2+Au_3]^+$ was also observed with signal intensity $2.5 \cdot 10^3$. Arginine (Fig. 2C), had the highest S/N ratio (294) for $[C_6H_{14}N_4O_2+H]^+$ adduct with *m/z* 175.1179. Lysine (Fig. 2D) was found on the mass spectrum in the form of five types of adducts: protonated, sodium and potassium as well as with $Au^+$ and $Au_3^+$ of which the protonated adduct had the highest signal intensity of $1.7 \cdot 10^5$. On the other hand,

lysine-gold adduct with chemical formula $[C_6H_{14}N_2O_2 + Au]^+$ with *m/z* 343.0651 had signal intensity of $1.1 \cdot 10^4$ and also trigold adduct $[C_6H_{14}N_2O_2 + Au_3]^+$ with *m/z* 737.0090 was found with signal intensity $6.1 \cdot 10^3$.

Alanine was analyzed on $^{109}$AgNPET target for LDI MS, presenting a spectrum with the higher intensity $1.2 \cdot 10^5$ for alanine-silver 109 adduct for concentration 50 ng per spot [37]. Nitta and coworkers detected arginine with the use of laser-based mass spectrometer at amount of 100 pmol with the use of PtNPs [38]. Lysine was analyzed on AuNPET target for LDI MS, presenting a spectrum with the intensity of $7.6 \cdot 10^4$ for protonated adduct for concentration 0.1 mg/mL. The mass spectrum also showed a gold adduct $[C_6H_{14}N_2O_2 + Au]^+$ with signal intensity of $3.0 \cdot 10^4$ [39].

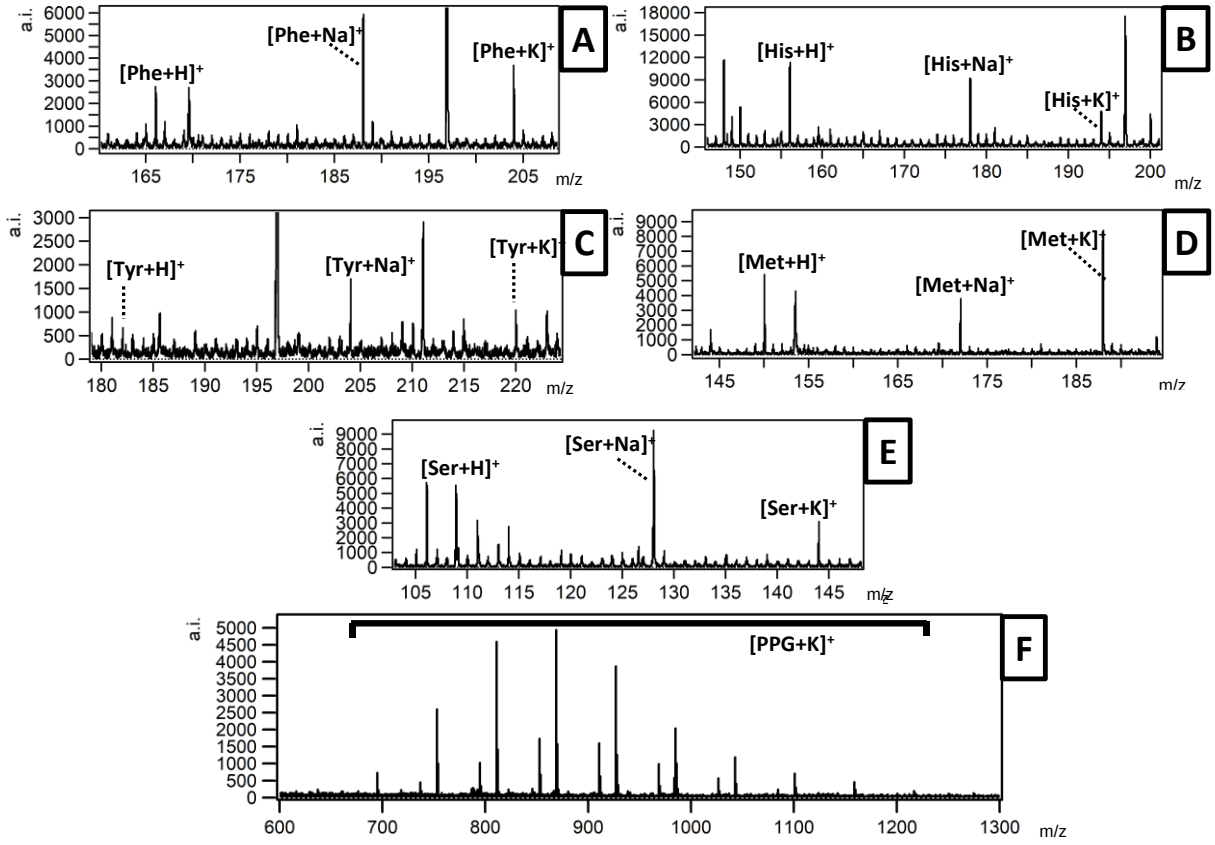


Fig 3. LDI MS positive reflectron mode mass spectra. Individual panels show fragment mass spectrum for A-phenylalanine, B-histidine, C-tyrosine, D-methionine, E-serine, respectively. The last panel (F) presents LDI MS spectrum of poly(propylene glycol) at 10.0 μg/mL concentration.

Figure 3 shows the fragments of the mass spectra obtained for phenylalanine, histidine, tyrosine, methionine, serine and poly(propylene glycol) using AuNPs LDI MS. No adducts of the tested compounds with gold ions were observed in any of the spectra in Fig. 3. For phenylalanine (Fig. 3A), tyrosine (Fig.3C) and serine (Fig. 3E) the highest signals were observed for $[C_9H_{11}NO_2+Na]^+$ adduct at *m/z* 188.0793 with signal intensity $4.5 \cdot 10^3$, $[C_9H_{11}NO_3+Na]^+$ adduct at *m/z* 204.0693 with signal intensity $1.0 \cdot 10^3$ and $[C_3H_7NO_3+Na]^+$ adduct at *m/z* 128.0789 with signal intensity $8.1 \cdot 10^3$. Sodium and potassium adducts were also present but with lower intensities. Histidine MS spectrum obtained with the use of PFL 2D GS LGN AuNPs is shown in Figure 3B. This compound was found mainly as protonated adduct $[C_6H_9N_3O_2 +H]^+$ with signal intensity of $8.9 \cdot 10^3$. On the other hand, on methionine (Fig. 3E) mass spectrum was dominated by potassium adduct $[C_5H_{11}NO_2S +K]^+$ at *m/z* 188.0242 with signal intensity $6.5 \cdot 10^3$.

Poly(propylene glycol) has repeating monomer unit of chemical formula $CH_2CH(CH_3)O$ with mass of approx. 57.9 Da. The LDI mass spectrum of PPG is shown in Fig. 3F. The spectrum show a typical

polymer structure where the dominant mass is approximately at *m/z* 1000. For example, the highest polymer signal at *m/z* 869 revealed is the $K^+$ ion adduct of a PPG with 14 mer units. Shoji Okuno et al. compared the PPG spectra obtained with MALDI and SALDI. The authors identified a problem with the reproducibility of the MALDI mass spectra for PPG, which showed a strong dependence on the type of solvent and/or chemical matrix and the analyte/matrix ratio [40].

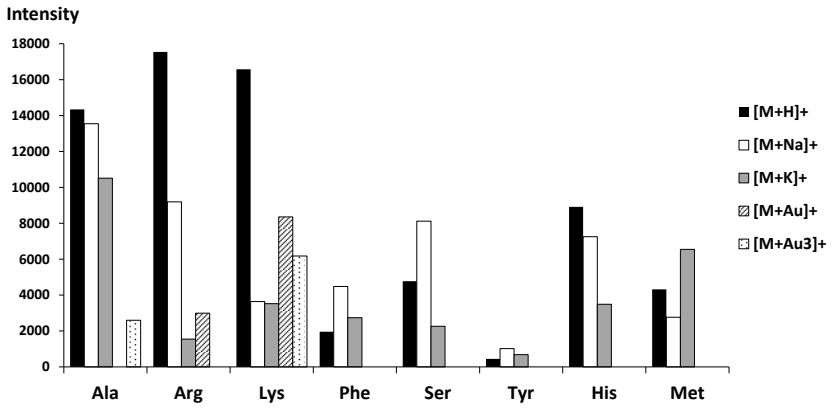


Fig 4. Signal intensity diagram for protonated, sodium, potassium, $Au^+$ and $Au_3^+$ adducts for individual amino acids.

Figure 4 contains bar chart of signal intensities for $H^+$, $Na^+$, $K^+$, $Au^+$ and $Au_3^+$ adducts for individual amino acids. Adducts with gold ions have been identified for only three amino acids: alanine, arginine and lysine. Proton, sodium and potassium adducts were detected on all mass spectra. For alanine, arginine, lysine and histidine, the proton adduct was the dominant adduct on the spectrum. On the other hand, the $Na^+$ adduct dominated in the LDI MS spectra of phenylalanine, serine and threonine.

### 2.2. Conclusions

Methods of synthesis and application of chemically pure monoisotopic gold nanoparticles onto studied surface for LDI MS was presented. Methodology was proven to be very useful for analysis of amino acids and also for characterization of low-mass polymers. Procedures shown are cost-effective, fast, efficient and instrument-limited.

## 3. Experimental

### 3.1. Materials

The gold foil (~ 1 mm thick) of 99.9% purity was bought from Polish Mint (Poland). Alanine, arginine, histidine, methionine, phenylalanine and serine were purchased from Sigma-Aldrich (99% purity). Lysine and tyrosine were purchased from Fluka Analytical Standards (98% purity). Poly(propylene glycol) (PPG, average Mn 1000 Da) was purchased from Sigma-Aldrich. All solvents were of HPLC grade, except for water (18 MΩ·cm water produced locally). Steel targets were machined from H17 (1.4016) stainless steel. Before the LDI MS experiments steel targets were cleaned through soaking in boiling solvents: toluene (3x100 mL, each plate for 30 s), chloroform (3x100 mL, each plate for 30 s), acetonitrile (3x100 mL, each plate for 30 s) and deionized water (3x100 mL, each plate for 30 s). Every plate was dried in high vacuum (ca. 0.01 mbar, 24h).

### 3.2. Methods

#### 3.2.1 PFL 2D GS Laser Generated Nanomaterial (LGN) of gold nanoparticles

The experimental arrangement for the AuNPs preparation by laser ablation is shown in Fig.1A. The gold foil was placed at the bottom of a glass vessel containing mixture solvents isopropanol and water (1:1 v/v). The Au foil was covered by an approximately 3 mm thick layer of mixture solvents (total solvent volume was 4 mL). The laser ablation was carried out with a 1064 nm pulsed fiber laser (Raycus RFL-P20QE/A3). Suspension was obtained after 2 min. irradiation with pulse energy of 0.7 mJ (100 ns

pulse length) at a 60 kHz repetition rate. Laser ablation was accomplished at a scanning speed of 5000 mm/s, the ablation area was 4x4 mm. Suspension was immediately transferred into a syringe and used in the nebulization step.

### 3.2.2 Nebulization of AuNPs suspension

The experimental setup for the nebulization of AuNPs suspension is shown in Fig.1B. The entire nanoparticle nebulization process was controlled by a computer. The H17 steel plate (laser mass spectrometry target plate) was placed on the table of a translation system consisting of a motorized XY table (EzM-42XL-A powered by closed-loop Ezi-SERVO motors). Glass syringe (1 mL) was filled with a previously prepared suspension of gold nanoparticles and placed in a syringe pump (pumping speed 250 μL/min). The custom-made software directed the 2D system table with 10 mm/s speed using a sequence of movement designed to uniformly cover a target plate. Nebulizer was obtained from Bruker Amazon ETD ESI ion source. Argon at a pressure of 2 bar was used as the nebulizing gas. Generally, all studied samples for MS were placed on the target plate before nebulization.

### 3.2.3 AuNPs characterization

AuNPs suspension was characterized by UV–VIS spectroscopy (Jasco V-670 spectrophotometer). Spectrum was registered in quartz cuvettes within 200–800 nm spectral range. The blank sample contained mixture solvents isopropanol and water (1:1 v/v). The suspension of AuNPs was also characterized by dynamic light scattering (DLS) using a Zetasizer-Nano ZS from Malvern Instruments. DLS measurements were performed by backscattering at a fixed detector angle of 173°. Isopropanol was used as dispersant.

### 3.2.4 LDI MS Experiments

Laser desorption/ionization – Time-of-Flight (LDI-ToF) mass spectrometry experiments were performed in reflectron mode using Bruker Autoflex Speed time-of-flight mass spectrometer equipped with a SmartBeam II laser (352 nm). Laser impulse energy was approx. 90-140 μJ, laser repetition rate 1000 Hz. The total number of laser shots was 4000 for each spot. This amount of laser shots was divided into four, symmetrically positioned points laying in distance of ca. 1/3 of spot radius from its center. At each point, 1000 laser shots were made with default random walk applied (random points with 50 laser shots). Measurement range was *m/z* 80-1500. Suppression was turned on typically for ions of *m/z* lower than 80. Reflector voltages used were 21 kV (the first) and 9.55 kV (the second). The data was calibrated and analyzed with FlexAnalysis (version 3.3) using centroid calibration model. Mass calibration (enhanced cubic calibration based on 7-8 calibration points) was performed using internal standards (gold ions $Au^+$ to $Au_5^+$).

### 3.2.5 LDI Sample Preparation

Solution (1 mg/mL) of each analyte was prepared by dissolving it in water (alanine, arginine, histidine, lysine, methionine, phenylalanine, serine and tyrosine). A solution of poly(propylene glycol) in isopropanol of 10 μg/mL concentration was prepared. A 0.5 μL volume of each of the final solution was applied to the steel target and air-dried followed by nebulization with AuNPs suspension.

### 3.2.6 High resolution scanning electron microscopy (HR SEM)

Target modified with AuNPs generated by PFL 2D GS method was inserted into the Helios Nanolab 650 electron microscope. Voltage was set at 10 and 30 kV, current was 0.2 nA. Images were made in nonimmersive mode.

**Acknowledgements**
Mrs. Małgorzata Walczak is acknowledged for DLS measurements. This work was supported by the National Science Centre (NCN), SONATA grant no. UMO-2018/31/D/ST4/00109.

## References

[1] Tanaka, K., Waki, H., Ido, Y., Akita, S., Yoshida,Y., Yoshida, T., Matsuo, T., *Rapid Commun. Mass Spectrom.* 1988, 2, 151–153.
[2] Egelhofer, V., Gobom, J., Seitz, H., Giavalisco, P., Lehrach, H., Nordhoff, E., *Anal. Chem.* 2002, 74, 1760–1771.
[3] Montaudo, G., Samperi, F., Montaudo, M.S., *Prog. Polym. Sci.* 2006, 31, 277-357.
[4] Wang, J., Zhao, J., Nie, S., Xie, M., Li, S., *Food Hydrocolloids* 2022, 124, 107237.
[5] Leopold, J., Popkova, Y., Engel, K., Schiller, J., *Biomolecules* 2018, 8, 173.
[6] Kołodziej, A., Płaza-Altamer, A., Nizioł, J., Ruman, T., *Int. J. Mass Spectrom.* 2022, 474, 116816.
[7] Domon, B., *Science* 2006, 312, 212–217.
[8] Berkenkamp, S., *Science* 1998, 281, 260–262.
[9] Shrivas, K., Wu, H-F., *Rapid Commun. Mass Spectrom*. 2007, 21, 3103–3108.
[10] Kołodziej A, Ruman, T., Nizioł, J., *J Mass Spectrom.* 2020, 55, e4604.
[11] Abdelhamid, HN., *Microchim Acta* 2019, 186, 682.
[12] Chiang, C-K., Chen, W-T., Chang, H-T., *Chem. Soc. Rev.* 2011, 40, 1269–1281.
[13] Sekuła, J., Nizioł, J., Rode, W., Ruman, T., *Anal. Chim. Acta* 2015, 875, 61–72.
[14] Herizchi, R., Abbasi, E., Milani, M., Akbarzadeh, A., *Artif Cells Nanomed Biotechnol* 2016, 44, 596–602.
[15] Khan, A., Rashid, R., Murtaza, G., Zahra, A., *Trop. J. Pharm Res* 2014, 13, 1169.
[16] Magro, M., Zaccarin, M., Miotto, G., Da Dalt, L., Baratella, D., Fariselli, P., Gabai, G., Vianello, F., *Anal Bioanal Chem* 2018, 410, 2949–2959.
[17] Xu, L., Wang, Y-Y., Huang, J., Chen, C-Y., Wang, Z-X., Xie, H., *Theranostics* 2020, 10, 8996–9031.
[18] McLean, JA., Stumpo, KA., Russell, DH., *J. Am. Chem. Soc.* 2005, 127, 5304–5305.
[19] Pilolli, R., Palmisano, F., Cioffi, N., *Anal Bioanal Chem* 2012, 402, 601–623.
[20] Amendola, V., Litti, L., Meneghetti, M., *Anal. Chem.* 2013, 85, 11747–11754.
[21] Płaza, A., Kołodziej, A., Nizioł, J., Ruman, T., *ACS Meas. Au* 2022, 2, 1, 14-22.
[22] Płaza-Altamer, A., Kołodziej, A., Nizioł, J., Ruman, T., *J Mass Spectrom* 2022;57 (3): .
[23] Rafique, M., Rafique, MS., Kalsoom, U., Afzal, A., Butt, SH., Usman, A., *Opt Quant Electron* 2019, 51, 179.
[24] Zulfajri, M., Huang, W-J., Huang, G-G., Chen, H-F., *Materials* 2021, 14, 11, 2937.
[25] Amendola, V., Meneghetti, M., *Phys. Chem. Chem. Phys.* 2009, 11, 3805.
[26] Ruman, T., Długopolska, K., Jurkiewicz, A., Rut, D., Frączyk, T., Cieśla, J., Leś, A., Szewczuk, Z., Rode, W., *Bioorg. Chem.* 2010, 38, 74–80.
[27] Arendowski, A., Ossoliński, K., Ossolińska, A., Ossoliński, T., Nizioł, J., Ruman, T., *Adv Med Sci* 2021, 66, 326–335.
[28] Arendowski, A., Ossoliński, K., Nizioł, J., Ruman, T., *Int. J. Mass Spectrom* 2020, 456, 116396.
[29] McLean, JA., Stumpo, KA., Russell, DH., *J. Am. Chem. Soc.* 2005, 127, 5304–5305.
[30] Abdelhamid, HN., Wu, H-F., *Anal Bioanal Chem* 2016, 408, 17, 4485–4502.
[31] Daruich De Souza, C., Ribeiro Nogueira, B., Rostelato, MECM., *J. Alloys Compd* 2019, 798, 714–740.
[32] Slepička, P., Slepičková Kasálková, N., Siegel, J., Kolská, Z., Švorčík, V., *Materials* 2019, 13, 1.
[33] Su, C-L., Tseng, W-L., *Anal. Chem.* 2007, 79, 4, 1626–1633.
[34] Haiss, W., Thanh, NTK., Aveyard, J., Fernig, DG., *Anal. Chem.* 2007, 79, 4215–4221.
[35] Amendola, V., Meneghetti, M., *J. Phys. Chem. C* 2009, 113, 11, 4277–4285.
[36] Dufresne, M., Thomas, A., Breault-Turcot, J., Masson, J-F., Chaurand, P., *Anal. Chem*. 2013, 85, 3318–3324.
[37] Arendowski, A., Nizioł, J., Ruman, T., *J. Mass Spectrom.* 2018, 53, 369–378.
[38] Nitta, S., Kawasaki, H., Suganuma, T., Shigeri, Y., Arakawa, R., *J. Phys. Chem. C* 2013, 117, 238–245.
[39] Arendowski, A., Ruman, T., *Anal. Methods* 2018, 10, 45, 5398–5405.
[40] Okuno, S., Wada, Y., Arakawa, R., *Int. J. Mass Spectrom* 2005, 241, 43–48.

*Article received: September 2022*
*Article accepted: October 2022*